Prism coupling technique for characterization of the high refractive index planar waveguides

V. PRAJZLER[a*], P. NEKVINDOVA[b], M. VARGA[c], J. BRUNCKO[d], Z. REMES[c], A. KROMKA[c]
[a]Dept. of Microelectronics, Faculty of Electrical Engineering, Czech Technical University, Technicka 2, 168 27 Prague, Czech Republic
[b]Institute of Chemical Technology, Technicka 5, 166 27 Prague, Czech Republic
[c]Institute of Physics, Academy of Sciences of the Czech Republic, v.v.i., Cukrovarnicka 10/112, 162 53 Prague 6, Czech Republic
[d]International Laser Centre, Ilkovicova 3, 841 04 Bratislava, Slovak Republic

We present the study of properties of semiconductor optical planar waveguides fabricated from materials with high refractive index. The nanocrystalline diamond and nanocrystalline zinc oxide planar waveguides have been deposited by microwave plasma enhanced chemical vapour deposition and by pulse laser deposition on glass substrates. Monocrystalline gallium nitride planar waveguides were prepared by metalorganic chemical vapour deposition on sapphire substrates. The morphology of prepared layers was characterized using scanning electron microscopy, Raman spectroscopy and X-ray diffraction. Waveguiding properties and the refractive indices of prepared thin films were determined by prism coupling technique and our measurement shows that our samples had waveguiding properties for all measured wavelengths from ultraviolet to infrared spectral range.

(Received June 17, 2016; accepted November 25, 2016)

Keywords: High index contrast, Optical planar waveguides, Zinc oxide, Nanocrystalline diamond, Gallium nitride

1. Introduction

Optical materials with high refractive index contrast (HIC) attracts considerable attention for photonic applications because they allow realization of complex optical waveguides interconnections, optical bends and S bend with lower radius and thus enable implementation of photonic structures with high density integration [1-3]. HIC waveguides can be divided into three types depending on the refractive indices (*n*) of the core and surrounding materials: (i) silicon (n = 3.5) deposited on a silica-on-silicon insulator [4, 5], (ii) moderate high index material with the core index around 2 [6, 7], such as Ta_2O_5 (n = 2.3) or SiON with high SiN content (n = 1.75-1.9) and (iii) polymer materials (n = 1.5) that were developed during the last decade and benefit from easy fabrication process and low cost [8, 9].

Novel materials which are suitable for the preparation of HIC waveguides are the nanocrystalline diamond (NCD), zinc oxide (ZnO) and gallium nitride (GaN). The advantages of the NCD are high refractive index (2.388 at 1311 nm), chemical and radiation inertness, high band gap (5.5 eV), high thermal conductivity, high density, large Young's modulus and high stability under extreme operating conditions [10, 11]. On the other hand, GaN and ZnO are direct wide-bandgap semiconductors (3.4 eV GaN, 3.3 eV ZnO) where, GaN belongs to III-V and ZnO to II-VI semiconductor groups. Semiconductors belonging to these groups possess several favorable properties, including good transparency, high electron mobility, room-temperature luminescence and also high value of refractive index (GaN 2.323, ZnO 1.932 both at 1311 nm). Such unique optical properties make them interesting for photonic applications and therefore they have been intensively studied during last decades by a lot of research groups [12-16 and references therein].

This paper deals with fabrication, characterization and measurement/comparison of the waveguiding properties of three different types of HIC optical planar waveguides. We are going to present and compare the waveguide properties of three different HIC materials: a) nanocrystalline diamond (NCD), b) zinc oxide (ZnO) and c) gallium nitride (GaN). The waveguiding properties of the as deposited thin films were investigated by prism coupling technique in TE polarization for five different wavelengths (473, 632.8, 964, 1311 and 1552 nm). Scanning electron microscopy (SEM), Raman spectroscopy and X-ray diffraction measurements were used to determine the morphology, chemical composition and crystallographic orientation of thin films.

2. Experiments

2.1. Preparation of the samples

The NCD and ZnO thin films were deposited on borosilicate glass substrates of sizes 10×10×0.1 mm^3 and 12×38×0.1 mm^3, respectively. Prior to deposition of NCD and ZnO films we calculated the minimal thickness of the film needed for guiding at least one optical mode of light (see subsection 3.1 and Tab. 1).

Before the diamond growth, the substrates were seeded by applying an ultrasonic agitation in water-diluted diamond colloid (NanoAmando Aqueous Colloid: Dispersed 5 nm Bucky diamond, 5.0 w/v%, Vol: 100 ml, with a median diamond grains size of 4.8 ± 0.6 nm (98.8 wt.%) and particle density of 288 quadrillion particles per 1 ml). Diamond films were grown in pulsed linear antenna microwave plasma chemical vapor deposition (CVD) process (modified system AK 400, Roth and Rau, AG) from the $CH_4/CO_2/H_2$ gas mixture [17]. The diamond growth was performed for 30 hours at a constant total gas pressure of 10 Pa at 2.5% of CH_4 and 10% of CO_2 in hydrogen, microwave power of 2×2 kW and substrate temperature of 650°C.

The thin ZnO films were prepared by Pulsed Laser Deposition (PLD) from pure ZnO target at room temperature. The target was sintered from fine grained ZnO powder without any doping (purity > 99.99%). The pulsed laser for ablation was Nd:YAG laser at THG (355 nm) with 10 Hz repetition frequency and 15 ns of pulse length (FWHM). The laser fluency was at constant level of 2.8 $J.cm^{-2}$ for all the samples and the thickness of ZnO layers was controlled by deposition time (33:20 minutes or 66:40 minutes respectively). Substrates (Eagle 2000 glass) were cleaned in ultrasonic bath in acetone for 5 minutes and subsequently preserved in 2-propanol. The deposition chamber was filled by pure oxygen atmosphere (O_2, purity 5.0) at 5 Pa pressure. The distance “target – substrate” was 67 mm.

The GaN thin film with the thickness of 6.1 μm was deposited on sapphire (Al_2O_3) substrate using a Metal Organic Chemical Vapor Deposition MOCVD (Technologies and Devices International, Inc.-TDI).

2.2. Materials characterization

The surface morphology of the deposited films was measured by scanning electron microscopy (SEM), employing e_LiNE writer (Raith GmbH) or FE-SEM Tescan MAIA 3. Raman spectra of the fabricated samples were acquired by Renishaw InVia Reflex Raman spectrometer equipped with the excitation wavelength of 442 nm. The crystallographic orientation of the films was determined by X-ray diffraction (XRD) spectroscopy. The X-ray diffractions were performed using the PANalytical high-resolution X-ray diffractometer Expert Pro Θ-Θ equipped with a parafocusing Bragg-Brentano geometry using CoKα radiation (λ= 1.78892 Å, U = 35 kV, I = 40 mA). The measurements were performed under ambient atmosphere. The measured data were evaluated with the software package High Score Plus. Waveguiding properties of the prepared NCD, ZnO and GaN optical planar waveguides were measured by dark mode spectroscopy using prism coupling technique (Metricon model 2010 prism coupler [18]) for transverse electric (TE) polarizations at five wavelengths 473, 632.8, 964, 1311 and 1552 nm. The measurements were done using two types of prism: i) Metricon #200-P-2-60 (n(measuring range) = 2.00–2.65, λ= 633 nm) and ii) #200-P-2 (n(measuring range) = 1.55–2.45, λ= 633 nm). The principle of this technique is available in [19, 20].

3. Results

3.1. Theoretical calculation and experimental evaluation of the films thickness

Step-index planar waveguide consists of a high-index dielectrical layer surrounded by lower refractive index material. Symmetrical optical waveguide has equal refractive index at both, substrate and cover material. However, as our waveguides will be asymmetrical, the index of refraction of the core waveguide n_1 must be higher than the refractive index of the substrate n_2 and that of cover material n_3. In the waveguiding layer there will be formed a standing wave based on the principle of transverse resonance from which a dispersion equation (1) can be derived:

$$\frac{2\cdot\pi}{\lambda_0}\cdot h\cdot\sqrt{n_1^2-n_{eff}^2} = \arctan\left(p_{12}\cdot\sqrt{\frac{n_{eff}^2-n_2^2}{n_1^2-n_{eff}^2}}\right)+\arctan\left(p_{13}\sqrt{\frac{n_{eff}^2-n_3^2}{n_1^2-n_{eff}^2}}\right)+k\cdot\pi \quad (1)$$

where λ_0 is the operating wavelength, h is thickness of the planar waveguide, n_1 is refractive index of the core layer, n_2 is refractive index of the substrate, n_3 is refractive index of the cover layer, n_{eff} is effective refractive index, k is an integer number k = 0, 1, 2 …. The p_{12} and p_{13} are defined for the TE mode as:

$$p_{12} = p_{13} = 1 \quad (2)$$

and for the TM mode as:

$$p_{12} = \left(\frac{n_1}{n_2}\right)^2 \quad , \quad p_{13} = \left(\frac{n_1}{n_3}\right)^2 \quad (3)$$

From the solution of the dispersion equation (1) follows description of the properties of the pertinent planar waveguides, as the critical thickness h_f (equation 4) of the optical planar waveguide and number of guided modes m (equation 5) [21, 22]:

$$h_f = \frac{\lambda_0}{2\cdot\pi\cdot\sqrt{n_1^2-n_2^2}}\left(k\cdot\pi + arctg\left(p_{13}\sqrt{\frac{n_2^2-n_3^2}{n_1^2-n_2^2}}\right)\right) \quad (4)$$

$$m = Int\left(\frac{2}{\lambda_0}\cdot h_f\cdot\sqrt{n_1^2-n_2^2}-\frac{1}{\pi}\cdot arctg\left(p_{13}\sqrt{\frac{n_2^2-n_3^2}{n_1^2-n_2^2}}\right)\right) \quad (5)$$

The next important parameter for optical waveguides for high density integration is the relative index difference Δ. The definition of relative index difference Δ is given by the equation 6:

$$\Delta = \frac{n_1^2 - n_2^2}{2 \cdot n_1^2} \quad (6)$$

where n_1 is refractive index of the core and n_2 is refractive index of the cladding. This definition implies that value of Δ is always lower than 50% [5]. Optical waveguides with the index difference higher than 20% are called high index contrast (HIC) optical waveguides.

Table 1 summarizes the tabular data of the refractive indices of the used substrates (Eagle glass and sapphire) and investigated materials (diamond, zinc oxide and gallium nitride). These values were used for the theoretical calculation of the minimal critical film thickness (h_f) of the waveguide, i.e. NCD, ZnO and GaN films, and the relative index difference Δ.

Table 1. Tabular data of the refractive indices used for the calculation [23].

Wavelength (nm)	Refractive index (-)				
	Eagle glass	Al_2O_3	Diamond	ZnO	GaN
473	1.523	1.777	2.439	2.077	2.464
632.8	1.515	1.766	2.412	1.989	2.385
964	1.508	1.756	2.394	1.945	2.339
1311	1.504	1.750	2.388	1.932	2.323
1552	1.501	1.746	2.386	1.927	2.317

The calculated data of the minimal film thickness (first four TE modes) for NCD, ZnO and GaN are listed for five different wavelengths (473, 632.8, 964, 1311 and 1552 nm) in Table 2.

Our results show that the minimal thickness of the film to guide at least one optical mode for all wavelengths should be at least 0.072, 0.152 and 0.122 μm for NCD, ZnO and GaN, respectively. The estimated average values of the relative index difference Δ for five investigated wavelengths are 30, 21 and 22% for glass/NCD, glass/ZnO and sapphire/GaN planar waveguides, respectively. All three calculated values fulfill the main requirement for HIC optical waveguides.

Table 2. Calculated minimal film thickness for optical planar waveguides based on NCD, ZnO and GaN

Wavelength (nm)	TE modes	Thickness of the planar waveguide h_f (μm)		
		Glass NCD	Glass ZnO	Al_2O_3 GaN
473	TE_0	0.021	0.036	0.031
	TE_1	0.146	0.204	0.170
	TE_2	0.270	0.371	0.308
	TE_3	0.394	0.539	0.447
632.8	TE_0	0.029	0.057	0.046
	TE_1	0.198	0.302	0.244
	TE_2	0.366	0.548	0.441
	TE_3	0.535	0.793	0.638
964	TE_0	0.045	0.093	0.075
	TE_1	0.304	0.485	0.387
	TE_2	0.563	0.878	0.699
	TE_3	0.823	1.270	1.010
1311	TE_0	0.061	0.129	0.103
	TE_1	0.414	0.669	0.532
	TE_2	0.768	1.210	0.961
	TE_3	1.121	1.750	1.390
1552	TE_0	0.072	0.152	0.122
	TE_1	0.491	0.794	0.632
	TE_2	0.909	1.435	1.141
	TE_3	1.746	2.077	1.651

3.2. Morphology and structure of the prepared films

The as-deposited films were characterized in terms of their morphology, chemical composition and crystallinity. The SEM images, Raman and XRD spectra of the NCD, ZnO and GaN films of the samples are shown in Figure 1.

NCD films: From the SEM image it is obvious that the diamond grains are faceted and their size varied up to 300 nm. Raman spectrum of the NCD film exhibits three characteristic peaks at 1150 cm^{-1}, 1332 cm^{-1} and 1585 cm^{-1}. The peak centered at 1332 cm^{-1} is a well known diamond peak and it is related to sp^3 hybridized carbon phases. The wide band centered at around 1585 cm^{-1} is known as the G-band ("graphite-band") and is related to the sp^2 phases (i.e. amorphous phases) preferentially localized at grain boundaries. The band localized at approximately 1150 cm^{-1} is assigned to transpolyacetylene fragments and generally represents a signature of the nanocrystalline nature of the diamond film [24]. Debye-Scherrer ring from XRD measurement is uniform for reflection (111), which undoubtedly confirms that the diamond grains are randomly oriented (it is not shown). The XRD diffraction pattern (see Fig. 1a) shows two main peaks: a preferential peak at 51.8° which corresponds to (111) crystallographic orientation and a small peak at 90.4° which is related to (220) crystal orientation. From these two reflections the average size of the grains was estimated to be 368 nm. Since the substrate is an amorphous glass no additional reflection from the substrate was presented.

ZnO films: High-resolution SEM image (Fig. 1b) revealed ZnO film with fine grain polycrystalline nature, high grain density and a perfect preferential c-axis orientation (cross-section SEM image is not shown here). Well-aligned ZnO grains with a diameter up to 30 nm were observed after PLD at the room temperature. The Raman spectrum of the ZnO thin film exhibited five significant bands at 334, 438, 493, 581 and 1157 cm^{-1}. The modes at 334 and 438 cm^{-1} are assigned to [E2 (high)-E2 (low)] difference mode and E2 (high) mode of the hexagonal wurtzite structure, respectively. The strong peak located at 438 cm^{-1} is a characteristic feature for the wurtzite ZnO lattice and indicates a good crystallinity of the film [25]. The peak at 581 cm^{-1} is related to multiphonon process and corresponds to A1(LO) phonon mode. The position of this peak varies from 574 up to 591 cm^{-1} due to an anisotropic short-range forces in the uniaxial ZnO lattice. This shift is mainly influenced by the direction of the polarization field ξ to optical axis c [26]. In our case the ξ was perpendicular to c. The overtone of two acoustic phonon modes A1 and E2 is located at 1151 cm^{-1} [24]. The XRD diffraction peaks are located at 34.432 and 72.614 and corresponds to the reflection from (002) and (103) crystal planes, respectively [27]. The XRD pattern also confirms the hexagonal wurtzite structure with the lattice constants of: a = 3.249 Å and c = 5.2097 Å.

GaN film: The SEM micrograph, Raman and XRD spectra of the reference GaN film deposited on sapphire substrate are shown in Fig. 1c. The smooth surface with no evident grain boundaries expects the single crystalline character of GaN. Raman spectrum exhibits two characteristic peaks at 569 and 734 cm^{-1} which correspond to TO and LO phonon modes of the hexagonal wurtzite crystal structure, respectively. The XRD measurement clearly shows a sharp peak at 40.44° which corresponds to the (002) crystallographic orientation.

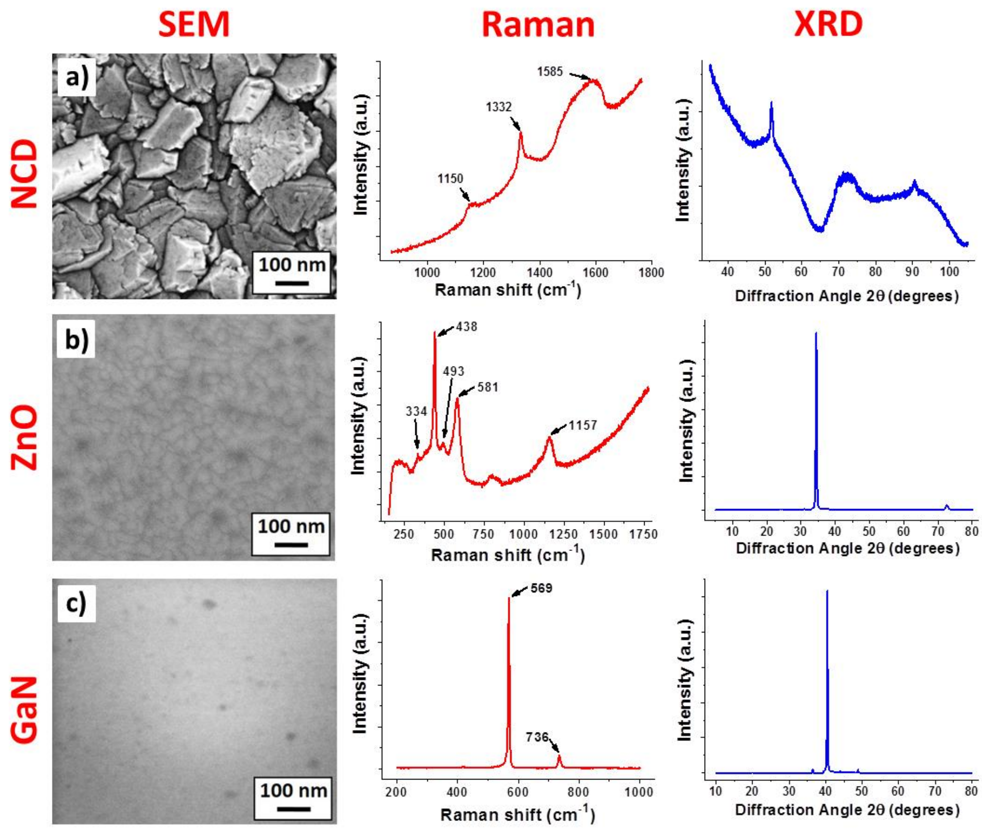

Fig. 1. SEM images, Raman and XRD spectra of the deposited NCD, ZnO and GaN films.

3.3. Waveguides measurement

The waveguiding properties of the deposited films were investigated in TE polarization for five different wavelengths (473, 632.8, 964, 1311 and 1552 nm). The sharp reflectivity dips at the angles correspond to the excitation of guided modes and can be attributed to the TE_0-TE_1 modes. The depth refractive index profiles were calculated for the samples/films where at least three optical modes were guided. The evaluation of the refractive index values for NCD, ZnO and GaN planar optical waveguides was done by prism coupling technique. The measured incident angles θ_c were substituted to the equation (7) and the refractive indices n were calculated for all the measured wavelengths (n_p is the refractive index of the used coupling prism) [22]:

$$\theta_c = \arcsin\left(\frac{n}{n_p}\right) \tag{7}$$

Using modelling software for the optical properties of thin films (Film Wizard™; Scientific Computing International, Carlsbad, CA, USA), the thickness (THK) of the NCD, ZnO and GaN films was evaluated from the interference fringes in the reflectance spectra that were measured in the visible and near infrared region. The calculated thickness for the NCD and ZnO films deposited on the glass was 280 and 460 nm, respectively. The THK of the GaN single crystal was about 6.1 µm. Based on theoretical calculations guiding of 3 optical TE modes should be expected for both NCD and ZnO films at the wavelength of 473 nm, 2 optical modes for 632.8 nm and 1 mode for 964, 1311 and 1552 nm. For the much thicker reference GaN film about 43 modes for 473 nm and more than 10 modes for the higher wavelengths (31 for 632.8 nm, 20 for 964 nm, 13 for 1311 nm and 12 for 1552 nm, respectively) are expected.

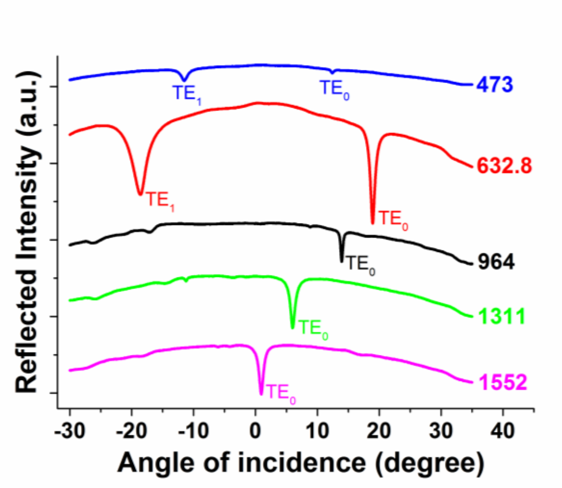

Fig. 2. The (TE) mode patterns for NCD optical planar waveguide measured at five wavelengths (473 nm, 632.8 nm, 964 nm, 1311 nm and 1552 nm).

NCD films: Fig. 2 shows measured (TE) mode patterns of the deposited NCD film with the thickness of 280 nm. The results showed that the NCD optical planar waveguide supported 2 TE modes at the wavelengths of 473 and 632.8 nm and 1 TE mode at 964, 1311 and 1552 nm. In comparison with the theoretically obtained results we observed only 2 guiding modes instead of 3 expected modes for the wavelength of 473 nm. This difference was caused by the used coupling prism range, i.e. such a prism allows seeing only 2 modes at this wavelength. For the higher wavelengths the coupling prism allows us to see all the expected guided modes. So the theoretically calculated values (Tab. 2) and obtained experimental results (Fig. 2) are in a good agreement.

ZnO films: Mode pattern measurements for ZnO (h = 460 nm) waveguides deposited on glass substrate determined that for the wavelengths of 473 and 632.8 nm the waveguide supported 2 modes, and for 964, 1311 and 1552 nm the waveguide supported 1 mode (see Fig. 3). According calculation result is one mode less for 473 nm. The reason could be lower optical power of the applied laser 473 nm and probably higher optical loss of ZnO at this wavelength. For the wavelengths above 632.8 nm the number of guiding modes also corresponds with our calculations (Table 2).

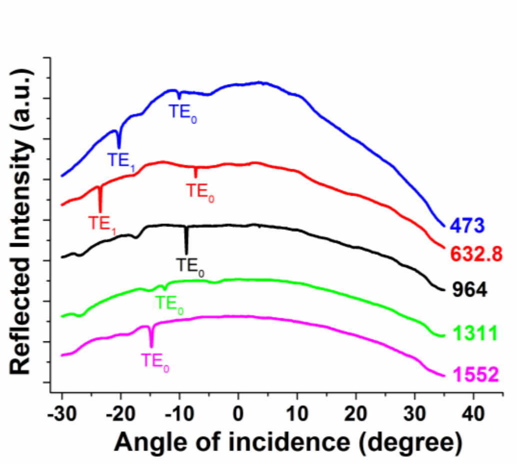

Fig. 3. The (TE) mode patterns for ZnO optical planar waveguide measured at five wavelengths (473 nm, 632.8 nm, 964 nm, 1311 nm, 1552 nm).

GaN film: The measured mode spectra of the GaN optical planar waveguide deposited on Al_2O_3 substrate are shown in Fig. 4. Because the thickness of the reference GaN film (h = 6.1 µm) is several times higher than NCD and ZnO films more than 20 modes were supported at the wavelengths of 437, 632.8 and 964 nm. For higher wavelengths the number of the supported modes was 12 at 1311 nm and 10 at 1552 nm.

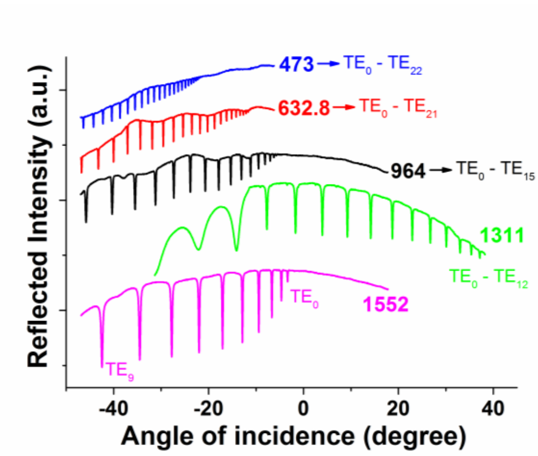

Fig. 4. The (TE) mode patterns for GaN optical planar waveguide measured at five wavelengths (473 nm, 632.8 nm, 964 nm, 1311 nm, 1552 nm).

The refractive index spectral dispersion for our planar optical waveguides was obtained by prism coupling measurement and compared to the theoretical dispersion curves for NCD, ZnO and GaN optical planar waveguides (see Fig. 5). For the ZnO film the measured refractive indices fit very well with the tabular one (see Tab.1). It indicates a high optical quality of the as-deposited ZnO film by the pulsed laser deposition. On the other hand, for both, NCD and GaN films the measured refractive indices were lower than to the tabular values (Tab. 2). In the case of NCD we explain this because of the polycrystalline character of the sample and the presence of the sp^2 hybridized phases on the grains boundary (see subchapter 3.2). A small difference of the refractive index in the case of the GaN film is less obvious and we speculate that it can be related to the imperfect single-crystalline nature and/or defects in the crystal structure.

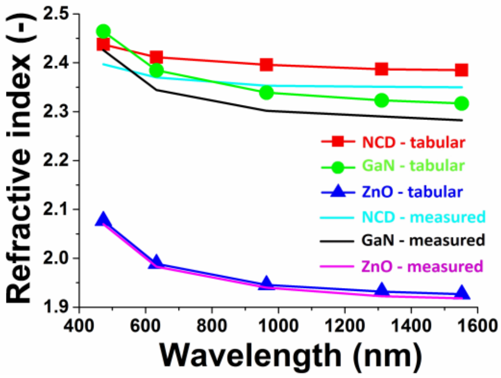

Fig. 5. Refractive indices of NCD, ZnO and GaN films at five wavelengths (473 nm, 632.8 nm, 964 nm, 1311 nm, 1552 nm) measured by prism coupling method (lines without symbols) and appropriate t abular values of the refractive indices (lines with symbols).

4. Conclusion

We investigated the high refractive index contrast optical planar waveguides based on the nanocrystalline diamond, ZnO and GaN. The morphology, chemical composition and crystallographic orientation of the prepared films were characterized by scanning electron microscopy, Raman spectroscopy and X-ray diffraction measurements and show a different structure and/or quality of the investigated materials. The waveguiding properties measured by prism coupling technique were confirmed for all the materials at five different wavelengths (473, 632.8, 964, 1311 and 1552 nm). Moreover, the values of refractive indices of the polycrystalline ZnO films are very close to tabular values. On the other hand, the values of refractive indices of NCD films are expectedly lower than tabular values because of the presence of the sp^2 hybridized phases on the grains boundary.

Furthermore, the estimated relative index difference Δ was 30, 21 and 22% for glass/NCD, glass/ZnO and sapphire/GaN planar waveguides, respectively. These high enough values of Δ together with unique properties of each of the material make such HIC waveguides suitable for tailored high density photonics circuits.

Acknowledgements

We gratefully acknowledge the Czech Science Foundation project GA14-05053S and Slovak Research and Development Agency project no. APVV-14-0716. This work was done within the LNSM infrastructure.

References

[1] C. Manolatou, S. G. Johnson, S. H. Fan, P. R. Villeneuve, H. A. Haus, J. D. Joannopoulos, Journal of Lightwave Technology **17**, 1682 (1999).
[2] B. E. Little, J. S. Foresi, G. Steinmeyer, E. R. Thoen, S. T. Chu, H. A. Haus, E. P. Ippen, L. C. Kimerling, W. Greene, IEEE Photonics Technology Letters. **10**, 549 (1998).
[3] V. Prajzler, P. Nekvindova, M. Varga, A. Kromka, Z. Remes, J. Optoelectron. Adv. M. **16**, 1226 (2014).
[4] A. Melloni, R. Costa, G. Cusmai, F. Morichetti, International Journal of Materials & Product Technology **34**, 421 (2009).
[5] Y. Kokubun, IEICE Trans. Electron. **E90-C**, 1037 (2007).
[6] B. E. Little, S. T. Chu, W. Pan, D. Ripin, T. Kaneko, Y. Kokubun, E. Ippen, IEEE Photonics Technol. Lett. **11**, 215 (1999).
[7] S. T. Chu, B. E. Little, W. Pan, T. Kaneko, S. Sato, Y. Kokubun, IEEE Photonics Technol. Lett. **11**, 691 (1999).
[8] A. Asael, Y. Glazer, M. Bin-Nun, D.M. Marom, IEEE Conference: Conference on Lasers and Electro-Optics (CLEO), Baltimore, 2011.
[9] T. Han, S. Madden, M. Zhang, R. Charters, B. Luther-Davies, Optics Express **17**, 2623 (2009).
[10] M. Varga, T. Izak, A. Kromka, M. Vesely, K. Hruska, M. Michalka, Central European Journal of Physics **10**, 218 (2012).
[11] M. Funer, C. Wild and P. Koidl, Appl. Phys. Lett. **72**, 1149 (1998).
[12] W. Junqiao, J. Appl. Phys. **106**, 011101 (2009).
[13] J. Bruncko, A. Vincze, M. Netrvalová, P. Šutta, M. Michalka, F. Uherek Applied Physics A-Materials Science & Processing **110**, 877 (2013).
[14] U. Ozgur, Y. I. Alivov, C. Liu, A. Teke, M. A. Reshchikov, S. Dogan, V. Avrutin, S. J. Cho, H. Morkoc, J. Appl. Phys. **98**, 041301 (2005).
[15] M. A. Reshchikov, H. Morkoc, Journal of Applied Physics **97**, 061301 (2005).
[16] S. J. Pearton, J. C. Zolper, R. J. Shul, F. Ren, J. Appl. Phys. **86**, 1 (1999).
[17] M. Varga, Z. Remes, O. Babchenko, A. Kromka, Physica Status Solidi B. **249**, 2635 (2012).
[18] Metricon Corporation: www.metricon.com
[19] R. Ulrich, R. Torge, Applied Optics **12**, 2901 (1973).
[20] V. Prajzler, P. Nekvindova, P. Hyps, V. Jerabek: J. Optoelectron. Adv. M. **17**, 1597 (2015).
[21] C. Pollock, M. Lipson: Integrated Photonics, Kluwer Academic Publishers 2003.

[22] V. Prajzler, P. Nekvindová, P. Hypš, O. Lyutakov, V. Jeřábek, Radioengineering **23**, 776 (2014).
[23] Refractive index database M. N. Polyanskiy. Refractive index database. Webpage http://refractiveindex.info.
[24] P. Galar, B. Dzurnak, M. Varga, M. Marton, A. Kromka, P. Maly, Opt. Mat. Exp. **4**, 624 (2014).
[25] R. Zhang, P.-G. Yin, N. Wang, L. Guo, Solid State Sciences **11**, 865 (2009).
[26] K. A. Alim, V. A. Fonoberov, M. Shamsa, A. A. Balandin, Journal of Applied Physics. **97**(12), 24313 (2005).
[27] F. Gu, S. F. Wang, M. K. Lu, G. J. Zhou, D. Xu, D. R. Yuan, Langmuir **20**, 3528 (2004).

*Corresponding author: xprajzlv@feld.cvut.cz